INFLUENCE OF AIR ENTRAPPMENT ON FLOOD EMBANKMENT FAILURE MECHANISM – MODEL TESTS

Piotr Bogacz[1], Jarosława Kaczmarek[1], Danuta Leśniewska[2]

[1] Department of Civil Engineering and Building Structures
University of Warmia and Mazury in Olsztyn
[2] Institute of Hydro-Engineering, Polish Academy of Sciences, Gdansk
Koszalin University of Technology, Koszalin

K e y w o r d s: flood embankment, air trapping, failure mechanism.

A b s t r a c t

The paper describes model tests on flood embankments, performed within the frame of EC 6th Framework Integrated Project FLOODsite (LEŚNIEWSKA et al. 2007). It is focussed mainly on presenting physical phenomena observed during the tests and related to air entrapment within embankment body and its subsequent release. The most important conclusion derived from recent tests is the existence of clear relationship between air entrapment and release and failure of internal embankment structure. Primary results of deformation of the embankment with a help of PIV analysis are also presented in the paper, showing air trapping influence on the embankment global failure mechanism.

WPŁYW ZAMYKANIA POWIETRZA NA MECHANIZM ZNISZCZENIA WAŁU PRZECIWPOWODZIOWEGO – BADANIA MODELOWE

Piotr Bogacz[1], Jarosława Kaczmarek[1], Danuta Leśniewska[2]

[1] Katedra Budownictwa i Konstrukcji Budowlanych
Uniwersytet Warmińsko-Mazurski w Olsztynie
[2] Instytut Budownictwa Wodnego PAN w Gdańsku,
Politechnika Koszalińska

S ł o w a k l u c z o w e: wały przeciwpowodziowe, zamykanie powietrza, mechanizm zniszczenia.

A b s t r a k t

Praca zawiera wyniki badań modelowych wału przeciwpowodziowego, przeprowadzonych w ramach zintegrowanego projektu 6 PR UE *FLOODsite* (LEŚNIEWSKA i in. 2007). Zaprezentowano

zjawisko fizyczne zaobserwowane w trakcie badań, związane ze zjawiskiem zamykania i uwalniania powietrza w korpusie wału. Najważniejszym wnioskiem wynikającym z dotychczasowych badań jest wyraźny związek między zamykaniem i uwalnianiem powietrza a niszczeniem wewnętrznej struktury wału. W pracy przedstawiono również wyniki wstępnej analizy przebiegu deformacji wału metodą PIV, która pozwoliła na zbadanie wpływu zamykania powietrza na uaktywnienie się globalnego mechanizmu zniszczenia wału.

Introduction

Flood embankments are very important from a safety point of view. They are mainly the earth structures and as such are intensively studied by soil scientists and engineers for many years. The history of flood embankments is quite long – in spite of this fact mechanisms of their internal structure failure and possible reasons of activating these mechanisms are still not recognised properly.

European Commission, within the framework of FLOODsite Integrated Project (2004-2009), addressed flood problems in a global way. One of the particular contributions to this project is the influence of air entrapped within a flood embankment on its failure mechanism. This particular problem is investigated from 2004 by common research team of Institute of Hydro-Engineering PAS in Gdańsk and University of Warmia and Mazury Civil Engineering Division. Within the frame of this cooperation a series of model tests were performed in Institute of Hydro-Engineering laboratory. The results of the tests are presented in this paper.

Test apparatus

The overall view of the test apparatus for model embankments is presented in Figure 1. It consists of the test box 200 cm long, 100 cm high and 4.5 cm wide, equipped with two transparent perplex walls, overflow device, gravel filter, vertically moving set of hoppers, enabling to form a model by sand pouring, pressure gauges mounted in the front perplex wall and connected to a computer recording system and water supply system (including rain generator).

The tests were recorded using digital cameras: SONY CYBERSHOT (2560 x 1920 pixels), HP PhotoSmart C850 (2272 x 1712 pixels) and PENTAX Optio T10, 2816 x 2112 pixels). During each test one of the cameras, named Camera 1, was covering the whole area of the test box (Fig. 2.), the other one (Camera 2) was located closer to the model to catch the details of deformation and produce a picture suitable for later image analysis (PIV).
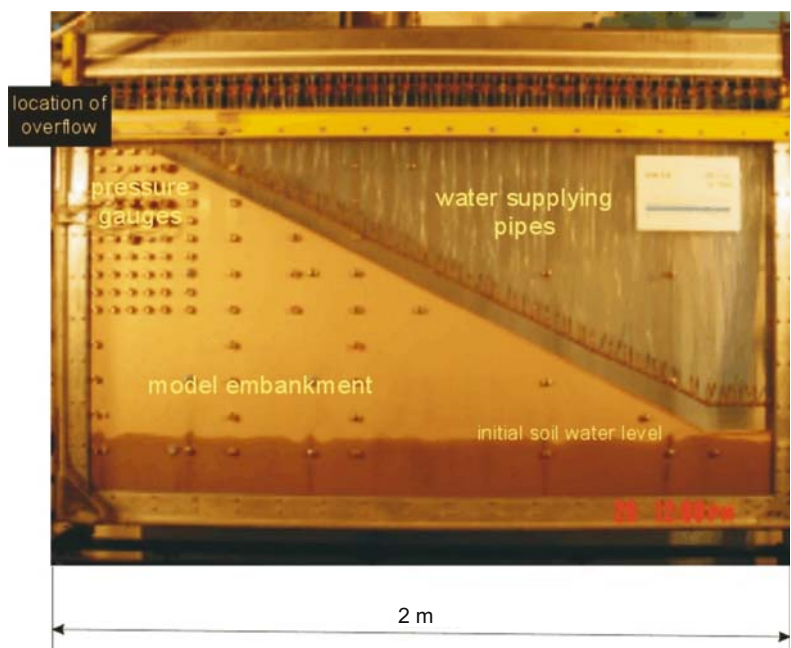
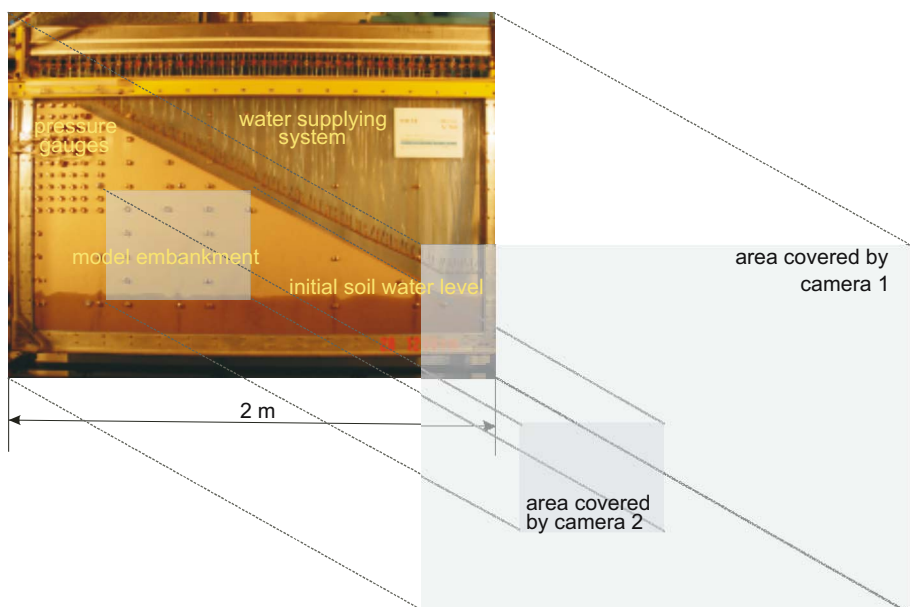Fig. 1. Model embankment in the test box

Fig. 2. Areas of the test box covered by Camera 1 and Camera 2

Sand used to build the embankment models was natural beach sand from Lubiatowo – a village placed 70 km north west from Gdańsk, at the open sea. It was a fine sand, characterised by d_{50} = 0.25 mm, well sorted. Results of sieve analysis made for this sand is presented in Table 1. Its water conductivity is k_s = 0.016 cm/s (ABO ELELA 1996), its initial moisture content 0.1% for all the tests performed. Sand built in a model was mostly in a dense state, characterised by average unit weight equal to 17.0 kN/m^3 and internal friction angle equal to 34°.

Table 1

Sieve analysis for Lubiatowo sand

Grain diameter (mm)	Sand fraction (%)	Summa (%)
0.50	0.072	0.072
0.40	0.684	0.756
0.315	9.328	10.084
0.25	28.060	38.144
0.20	28.360	66.504
0.16	26.224	92.728
0.10	6.940	99.668
0.08	0.272	99.940
< 0.08	0.060	100.000

Model embankments were formed by sand pouring (Fig. 3) in the following steps:

1. Installing and calibrating the pressure gauges.

2. Preparing proper amounts of sand to fill in 20 containers in 4 hoppers placed above the test box.

3. Pouring sand from hoppers to obtain the embankment model built of dense sand (Fig. 3).

4. Correction of the model profile with a help of special vacuum cleaner (if necessary).

5. Setting initial water table (Fig. 4).

Method of forming an embankment model by sand rain consists in pouring sand from hoppers from constant height (equal to 0.7 m in case of the tests presented in this paper), what can be achieved by vertical movement of the set of hoppers with constant speed. It was not possible to pour sand evenly in horizontal layers. The sand flow was sometimes turbulent, mainly due to apparent electric charge of sand grains, causing horizontal deviation of gravitational sand flow, what resulted in "waved" soil surface, far from horizontal. This effect was additionally strengthened by random to some extent character
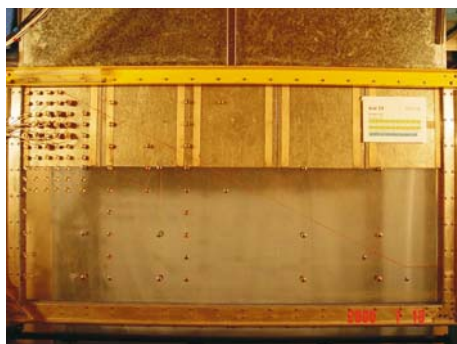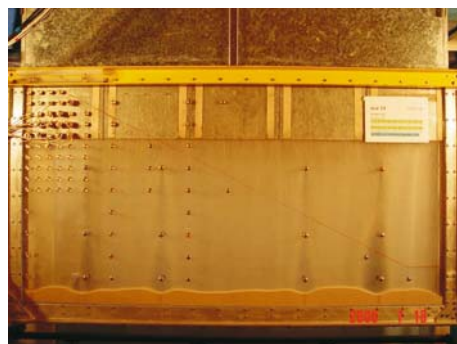
1 – *t* = 0, test 14, Phot. 2689, camera 1

2 – *t* = 3 min, Phot. 2692, camera 1

3 – *t* = 5 min, Phot. 2696, camera 1

4 – *t* = 7 min, Phot. 2700, camera 1

5 – *t* = 7.5 min, Phot. 2701, camera 1

6 – *t* = 8 min, Phot. 2702, camera 1

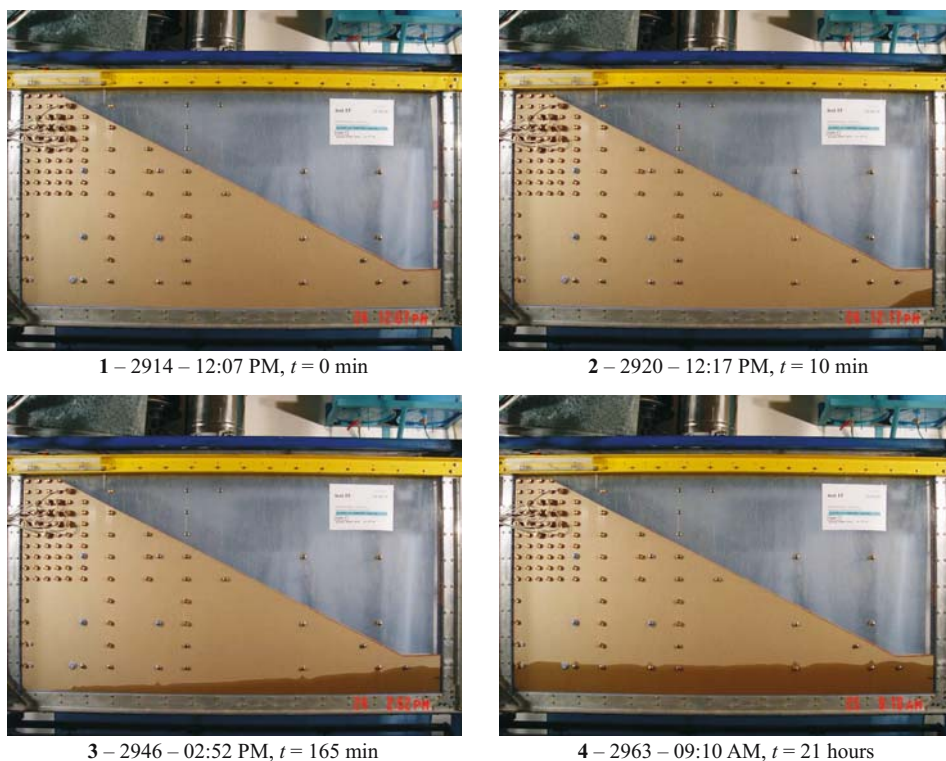Fig. 3. Example of building the embankment model by pouring (test 14)

1 – 2914 – 12:07 PM, $t = 0$ min

2 – 2920 – 12:17 PM, $t = 10$ min

3 – 2946 – 02:52 PM, $t = 165$ min

4 – 2963 – 09:10 AM, $t = 21$ hours

Fig. 4. Example of setting initial soil water table (Test 15)

of the flow from hoppers. As a result the internal structure of the embankment model was rather complex, but steady from test to test, giving not perfectly uniform, but highly repeatable internal structure of the model.

Setting of the initial water table was made through the inlet placed at the right down corner of the test box. The proper tests were performed 2-3 days after setting the initial soil water table. The tests were made on a model of landward embankment slope of inclination 1:2 , 0.8 m high and 1.60 m long. It was situated on a subsoil layer 0.2 m thick, made of the same sand. The width of the embankment crown was 0.2 m.

Two types of tests were performed, for which to ways of supplying water to the model were employed:

– **type A** – water supplied to the embankment body by rain generator, along the whole slope length. This type of test can simulate both conditions created by overflow (without significant surface erosion) and by heavy rainfall,

– **type B** – water supplied to the model from its top by rising water level in overflow vessel (real overflow).

Test results

Due to a big number of tests performed three representative tests were chosen to present typical results: test 14, test 15 and test 17. Data collected during these test illustrate best the process of air trapping and its influence on the embankment internal structure.

– Test 14 – type A test (rain generator used to supply water along the whole length of the embankment slope), intensity of water supply q ~ 10 ml/s.

– Test 15 – type B test (water supplied by overflow vessel from the top of the embankment model), q ~ 4 ml/s.

– Test 17 – type B test, q = 9.25 ml/s.

Original numbers given by the digital cameras are left in the photographs descriptions.

Test 14

Course of test 14 is shown in Figure 5. Photographs taken by the two cameras are put on together in this figure for the purpose of further analysis. The darker areas visible on photographs are wet, the lighter ones are dry. Several zones of entrapped air were created and lasted for some time during the test. Most of them disappeared in later stage of the test (air escaped to the atmosphere). At 22 min of water supplying to the embankment body the first traces of slope failure were noticed some distance from the toe of the model. Also about this moment the first cracks were observed to form and later open in isolated dry areas, surrounded by saturated soil.

Test 15

Course of the test 15 is presented in Figure 6. Water was supplied to the embankment not by the rain generator along the whole slope length, like it was in previous case, but from the top of the model by overflow vessel. Intensity of overflow was about 4 ml/s. For this intensity no air trapping occurred. Start of the slope failure was observed later than in case of test 14 (after 81 min), but its shape and location were similar.
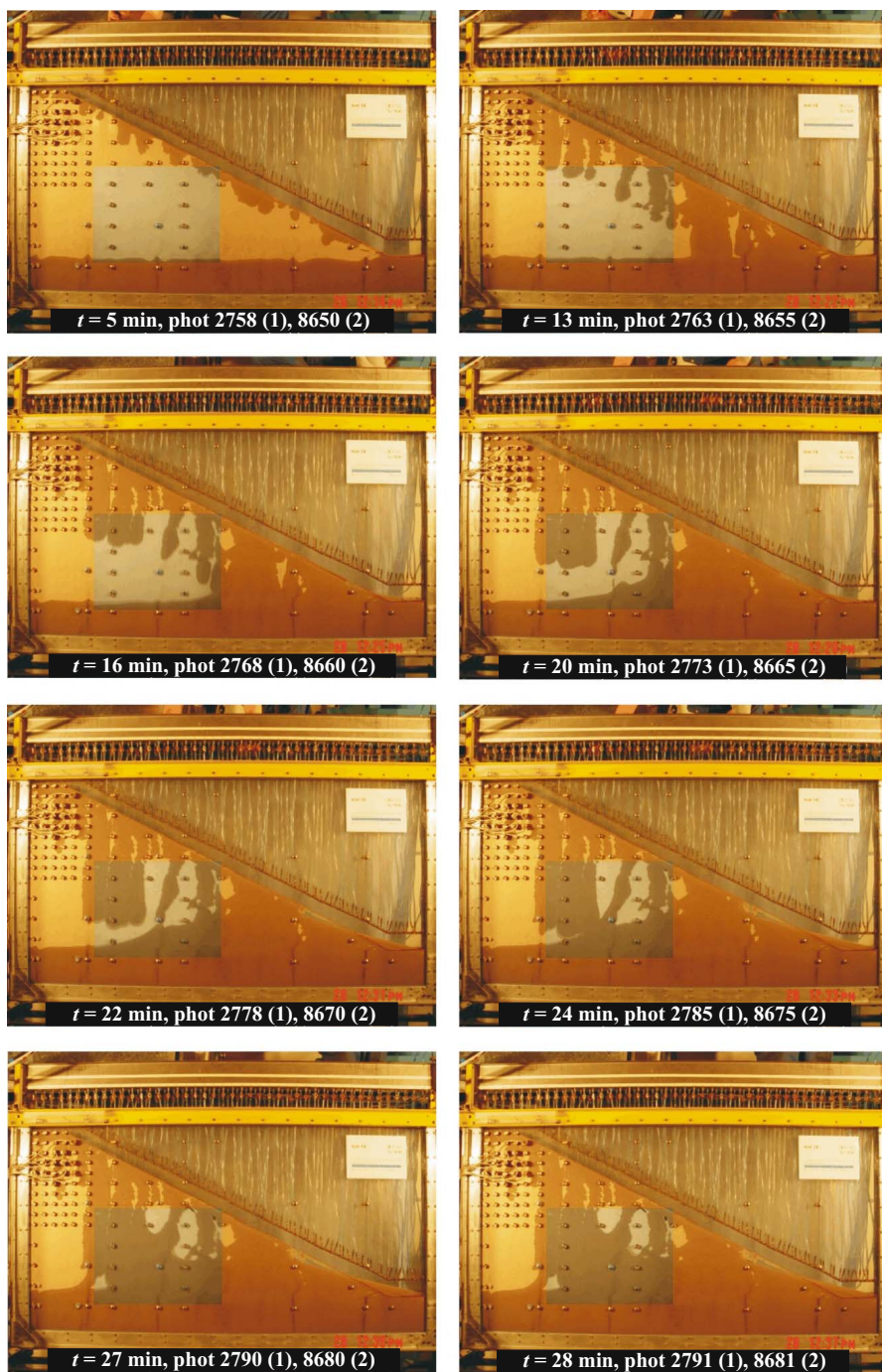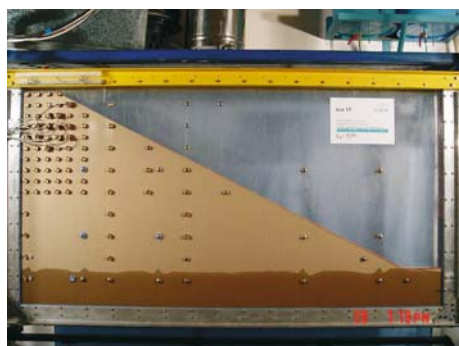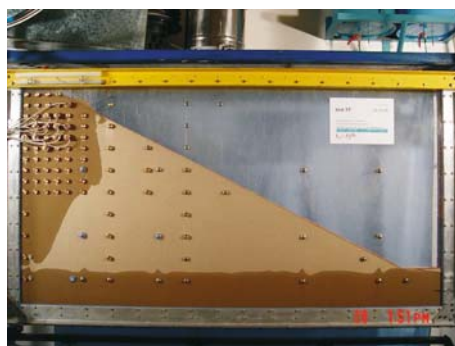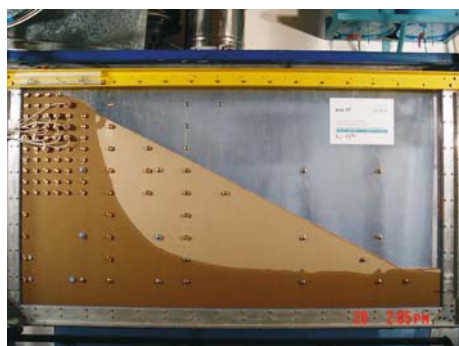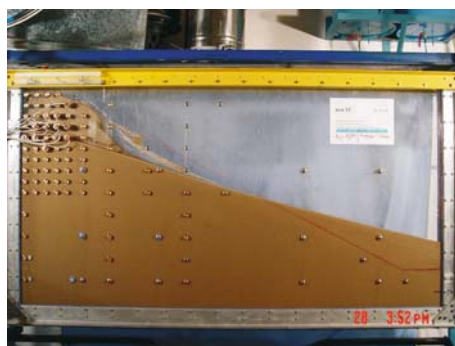
Fig. 5. Course of test 14

1 – 2968 – 01:19 PM, $t = 0$ min

2 – 2995 – 01:51 PM, $t = 32$ min

3 – 3007 – 02:05 PM, $t = 46$ min

4 – 3098 – 03:52 PM, $t = 153$ min

Fig. 6. Course of test 15

Test 17

Test 17 is presented in Figure 7. It was a repeat of test 15 with greater overflow intensity (q = 9.25 ml/s). Air entrapment occurred after 19 min of water supply. Some of the entrapped air zones resulted in cracks opening,. The opened cracks proved to be very stable and lasted even after drying an rising again water table.
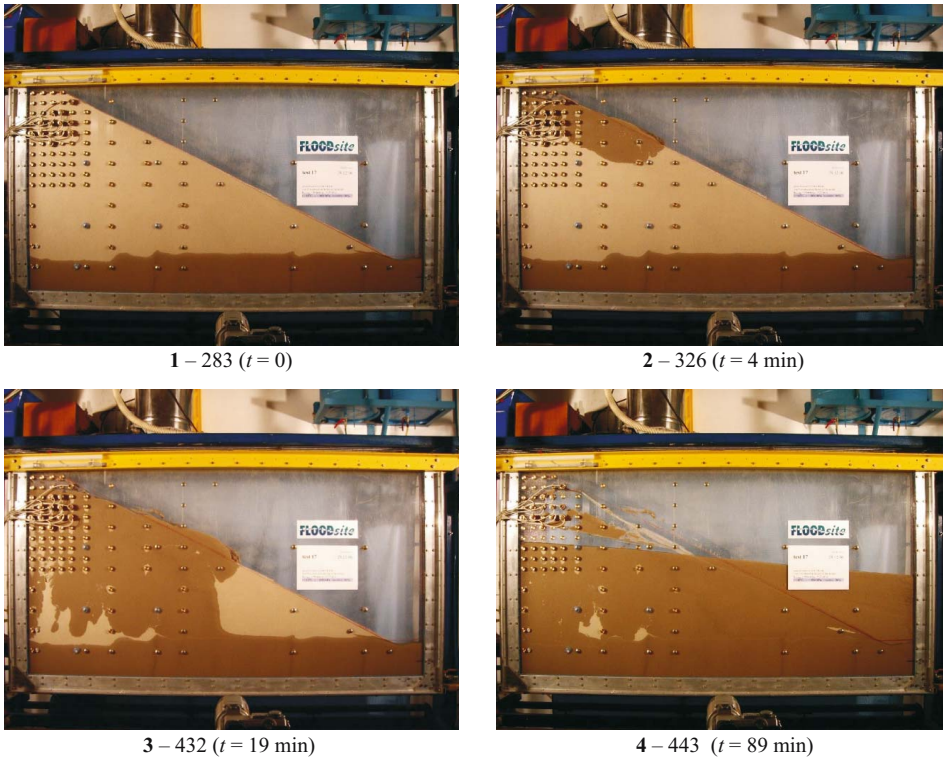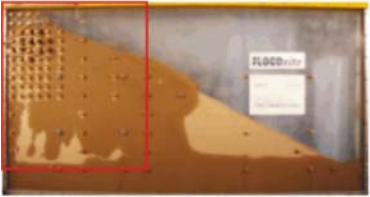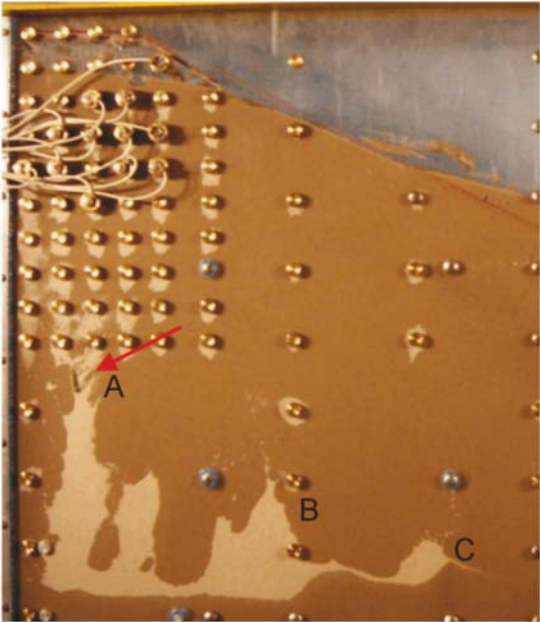

1 – 283 (t = 0)

2 – 326 (t = 4 min)

3 – 432 (t = 19 min)

4 – 443 (t = 89 min)

Fig. 7. Course of test 17

camera 1
phot. 433
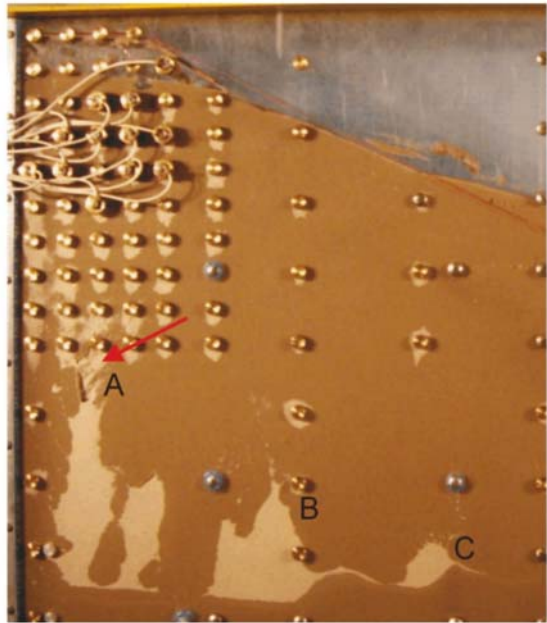t = 59 min (2)

camera 1
phot. 434
t = 60 min

Fig. 8. Example of entrapped air release

Analysis of the tests results

Two types of analysis were made on test 14 and test 17 data, for which air trapping occurred. The first was related to soil air pressure measurements, the second to deformations of model embankment during water infiltration.

Entrapped air pressures

Measuring entrapped air pressure was not easy, as the location of air entrapment was random and varied from test to test. It was expected however, on the basis of previous works (ZARADNY 1994, 1999, ABO ELELA 1996), that the most probable location for air entrapment was the area below the top of embankment and the pressure sensors were located there. This assumption proved to be true in most cases, but sometimes air was closed also in the central part of the model. In some cases rapid escape of air was observed, so sudden, that not possible to catch by a camera. Spectacular escape of air bubble accompanied by successful record of air pressures was observed during test 17 (Fig. 8). Comparison of pressure graphs and relevant photographs shows that air pressure changes reflect properly consecutive test stages. Stable parts of pressure graphs coincides with air bubble of stable dimensions, sudden pressure rises correspond to rapid air escape to the atmosphere.

Displacements and strain fields

Displacement and strain fields were analysed, using image processing software geoPIV, based on the PIV (particle image velocimetry) method. Preliminary results obtained for test 14 are presented in Fig. 9.

Conclusions

Measurements made during flood embankment tests proved that the entrapped air pressure is higher than atmospheric. The measured difference was about 25 hPa at peak. It was enough to induce internal cracks forming and opening within an embankment body.

Analysis of test results by the PIV method shows that the first measurable displacements and strains in flood embankment model can be observed already during setting the initial ground water level. It proves that ground water level variations introduce significant and irreversible changes of embankment
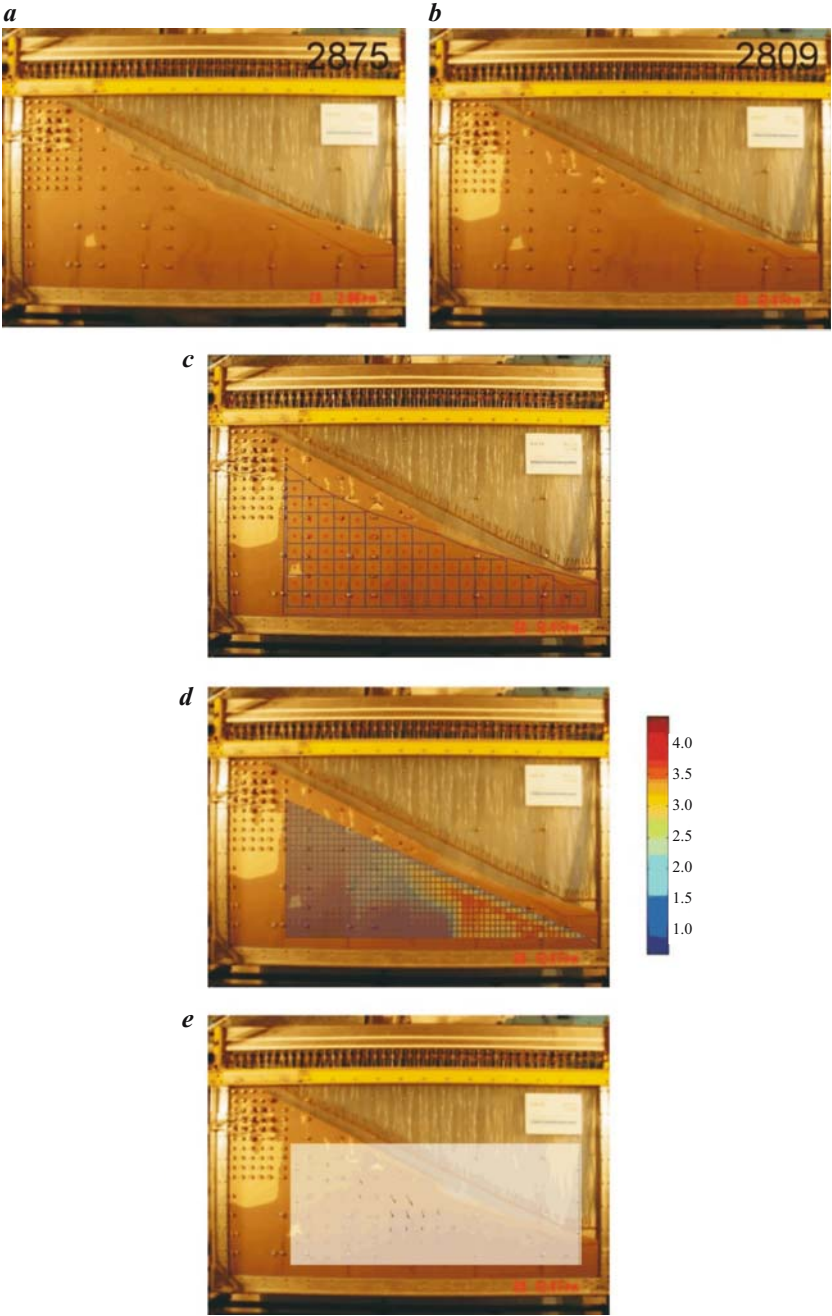
Fig. 9. Final failure displacements and strains – global failure mechanism

internal structure, which can in turn, in favourable conditions, activate global sliding embankment failure.

Acknowledgement

Disclaimer

This document reflects only the authors' views and not those of the European Community. This work may rely on data from sources external to the FLOODsite project Consortium. Members of the Consortium do not accept liability for loss or damage suffered by any third party as a result of errors or inaccuracies in such data. The information in this document is provided "as is" and no guarantee or warranty is given that the information is fit for any particular purpose. The user thereof uses the information at its sole risk and neither the European Community nor any member of the FLOODsite Consortium is liable for any use that may be made of the information.

References

ABO ELELA M.M.I. 1996. *Filtration phenomena in earth dike during intensive precipitation*. PhD Thesis, Polish Academy of Sciences, Institute of Hydro-Engineering, Gdańsk.

LEŚNIEWSKA D., BOGACZ P., KACZMAREK J., ZARADNY H. 2007. *Air trapping phenomenon and cracking*. FLOODsite Raport T04 07.

WHITE D.J., TAKE W.A. 2002. *GeoPIV: Particle Image Velocimetry (PIV) software for use in geotechnical testing*. Cambridge University Engineering, Department Technical Report, D-SOILS-TR322.

ZARADNY H. 1994. *Physical modelling of infiltration into dikes for stability purposes*. Road and Hydraulic Engineering Division, Rijkswaterstaat, Delft, Contract DWW-510 Final Report.

ZARADNY H. 1999. *Entrapped air – reason for the unexpected pore pressure behaviour in levees and earth dams*. Proceedings of XXVIII IAHR Congress – Hydraulic Engineering for Sustainable Water Resources Management at the Turn of the Millenium, Graz, Austria, pp. 7.